

Influence of carbon, manganese and nickel on microstructure and properties of strong steel weld metals

Part 3 – Increased strength resulting from carbon additions

E. Keehan^{*1}, L. Karlsson², H.-O. Andrén³ and H. K. D. H. Bhadeshia⁴

Neural network predictions suggested that the strength of a high strength steel weld metal with 7 wt-% nickel and 0.5 wt-% manganese could be increased significantly at moderate expense to impact toughness by additions of carbon. Based on this, three experimental weld metals were produced with carbon contents between 0.03 and 0.11 wt-%. Mechanical test results were in agreement with predictions. At low carbon content the microstructure was largely bainitic in dendrite core regions whereas martensite was found at interdendritic regions. From microstructural studies and dilatometry experiments it was found that carbon stabilised austenite to lower transformation temperatures and that the microstructure became more martensitic in nature. Effects on strength and impact toughness were explainable in terms of a refinement of the microstructure and tempering behaviour.

Keywords: High strength steel weld metal, Nickel, Manganese, Strength, Impact toughness, Carbon, Bainite, Martensite, Microstructure, Austenite, Transformation temperature, Tempering

Introduction

Welding research metallurgists have attempted to address the contradictory problems of higher strength, increased ductility, and good weldability without sacrificing impact toughness for shielded metal arc welding since the 1960s.¹⁻³ Following a trend of decreasing carbon concentration in high strength steel manufacture, the path of reducing carbon content was pursued, with carbon contents even lower than 0.01 wt-% tested.⁴ Weld metals with such low carbon content are largely dependent on other alloying elements such as manganese, nickel, chromium, and molybdenum for strength. They have good weldability and as alloying content or cooling rate is increased the microstructure becomes mainly bainite and martensite.

Recently, neural network modelling has been used as a development tool in many aspects of materials science. The advantages offered by this technique are described elsewhere.⁵⁻⁷ Using the composition of a commercial shielded metal arc welding electrode (ESAB OK 75-78, containing 3%Ni, 2%Mn, 0.5%Cr, 0.6%Mo, and 0.05%C – all wt-%)

as a starting point, it was predicted using neural network modelling that nickel must be added in a controlled manner with respect to manganese at a carbon content of 0.03 wt-%, otherwise impact toughness is greatly reduced.⁸ These predictions were confirmed experimentally and found to be in agreement with literature where similar compositions were studied.^{4,9} It was concluded from that work that to achieve both high strength and good impact toughness, the optimum alloying content of these elements was 0.5 wt-% manganese and 7 wt-% nickel.⁸ High resolution microstructural studies found the microstructure to be mainly upper and lower bainite, along with some martensite and a constituent previously unreported in weld metals, described as coalesced bainite.¹⁰⁻¹²

Manganese and nickel were set at their optimum values of 0.5 and 7.0%, respectively (all compositions are in wt-% unless stated otherwise), and the modelling was continued further for other alloying elements. It was predicted that strength could be increased at moderate expense to impact toughness by carbon additions as shown in Figs. 1 and 2.¹³ Three experimental weld metals were produced with carbon contents of 0.03, 0.06, and 0.11%. The present paper is the last in a series of three that investigate the effects of variations in alloying content of nickel,¹¹ manganese,¹⁰ and carbon in high strength steel weld metals. The present paper focuses on carbon, presenting results from high resolution microstructural investigations where the fine scale microstructure is characterised and links are made with the mechanical properties.

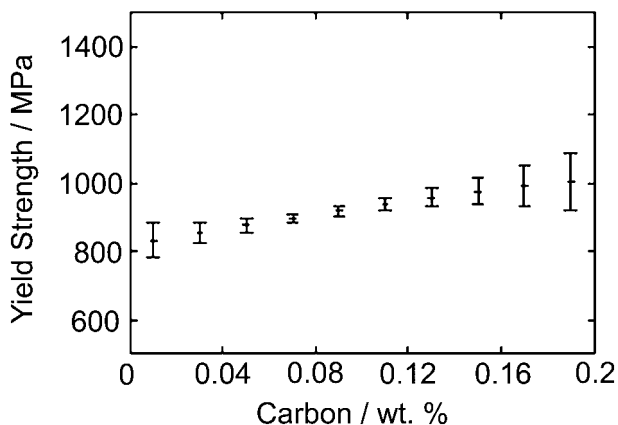
¹ESAB AB, PO Box 8004, SE-402 77 Gothenburg, Sweden. Work carried out in the Department of Applied Physics, Chalmers University of Technology, Kemigården 1, Fysikgränd 3, SE-412 96 Gothenburg, Sweden

²ESAB AB, PO Box 8004, SE-402 77 Gothenburg, Sweden

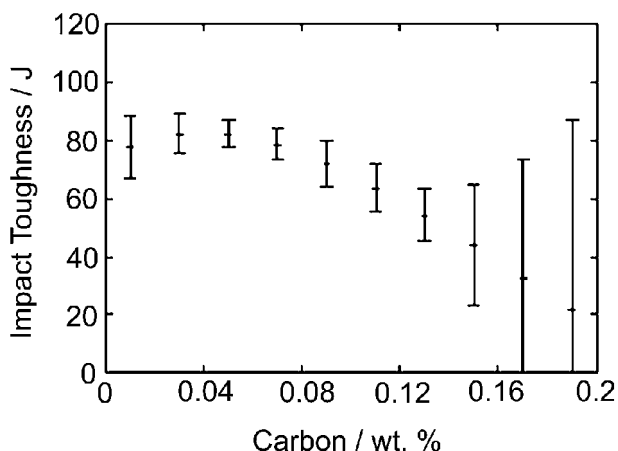
³Department of Applied Physics, Chalmers University of Technology, Kemigården 1, Fysikgränd 3, SE-412 96 Gothenburg, Sweden

⁴University of Cambridge, Department of Materials Science and Metallurgy, Pembroke Street, Cambridge CB2 3QZ, UK

*Corresponding author, email enda.keehan@esab.se



1 Predicted yield strength as function of carbon concentration for base composition of Fe-7Ni-0.5Mn-0.25Si-0.5Cr-0.62Mo: error bars represent $\pm 1\sigma$ uncertainty (after Ref. 13)

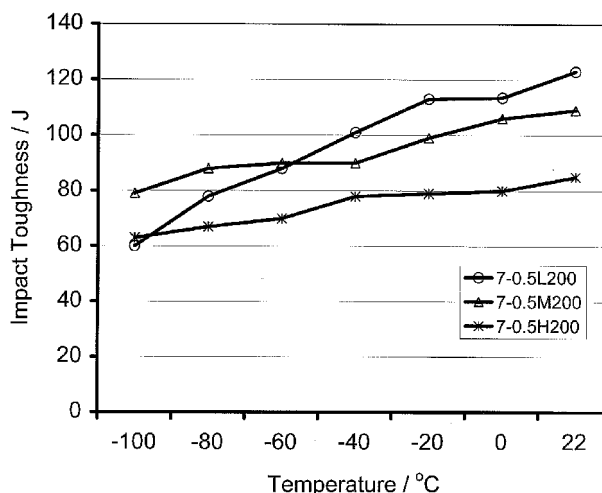


2 Predicted impact toughness at -60°C as function of carbon concentration for same base composition as in Fig. 1: error bars represent $\pm 1\sigma$ uncertainty (after Ref. 13)

Experimental procedures

The welded joints were made as described previously.¹¹ The welding parameters and chemical compositions are presented in Table 1. Weld metals were denoted 7-0.5L200, 7-0.5M200, and 7-0.5H200 where 7 represents the nickel content and 0.5 the manganese content, L, M, and H stand for the carbon contents (low, medium, and high), and 200 is the interpass temperature in $^{\circ}\text{C}$.

Specimens for Charpy V notch impact testing, tensile testing, dilatometry, and metallographic analysis (light optical microscopy (LOM), field emission gun scanning electron microscopy (FEGSEM), and transmission electron microscopy) were prepared as described



3 Charpy V notch impact toughness plots illustrating effect of increasing carbon content from 0.03 to 0.11 wt.-%

elsewhere.¹¹ Once microstructural studies were complete, hardness measurements were carried out on cross-sections using the Vickers method with a 10 kg load (HV10). In total 16 indents were made, starting in the last bead and proceeding down the centre of the welded joint in 1 mm steps.

Results

Mechanical properties

Tensile properties and Charpy impact toughness values are presented in Table 1 and Fig. 3, respectively. In short, it was confirmed that increasing carbon content from 0.03 to 0.11% increased yield strength from 777 to 912 MPa. In spite of this large increase in strength, impact toughness remained high with values of 78 J at -40°C and 63 J at -100°C being obtained for the weld metal with 0.11%C.

The results of hardness measurements are plotted in Fig. 4. As was expected, hardness increased with increasing carbon content. The hardness of the last bead increased by about 80 HV10, from approximately 320 to 400 HV10, as a result of changing the carbon content from 0.03 to 0.11%. On entering the central reheated regions a large decrease in hardness was experienced for all alloys, with weld metal 7-0.5H200 most strongly affected. In reheated regions the weld metals again followed the trend of higher hardness with greater carbon content.

Microstructure – last bead

Optical micrographs showing a fine scale microstructure are presented in Fig. 5. As is commonly found for high

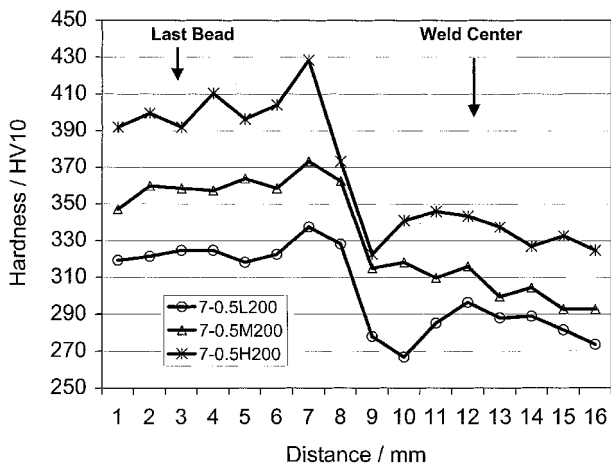
Table 1 Welding parameters, chemical composition (wt.-% except where indicated), and tensile properties

Weld metal	E, kJ mm^{-1}	IPT, $^{\circ}\text{C}$	$t_{8/5}$, s	C*	Si	Mn	P	S*	Cr	Mo	Ni	Cu	V	O, ppm*	N, ppm*	YS, MPa	UTS, MPa	YS/UTS	A_5 , %
7-0.5L200	1.3	200	10	0.030	0.4	0.61	0.010	0.009	0.16	0.38	6.11	0.02	0.018	340	150	777	831	0.94	22
7-0.5M200	1.4	200	11	0.061	0.34	0.56	0.011	0.006	0.15	0.35	6.84	0.01	0.014	350	160	858	895	0.96	18
7-0.5H200	1.3	200	10	0.110	0.38	0.53	0.008	0.007	0.14	0.40	7.04	NA	0.016	260	100	912	971	0.94	18

E energy input; IPT interpass temperature; $t_{8/5}$ estimated cooling time between 800 and 500°C calculated from WeldCalc;¹⁴ YS yield strength; UTS ultimate tensile strength; A_5 elongation.

NA not analysed.

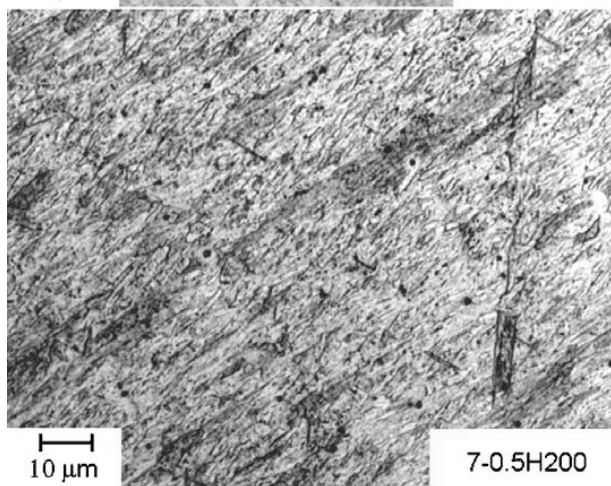
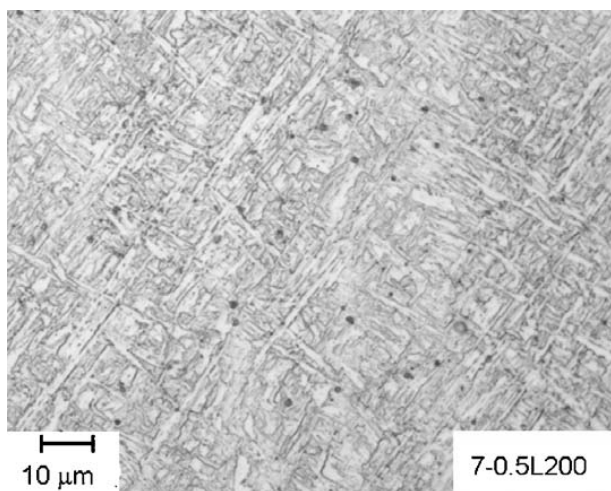
*Elements analysed using Leco Combustion equipment.



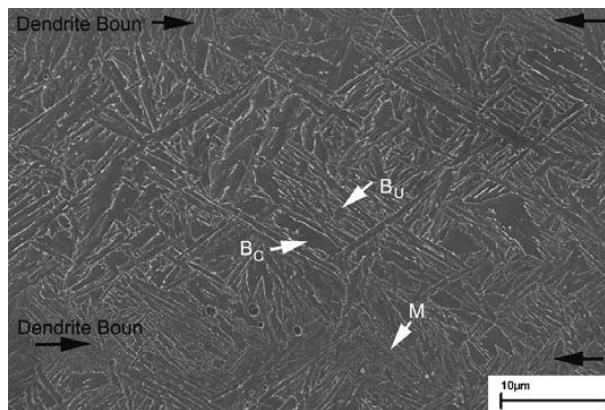
4 Hardness plots starting in last bead, showing effect of increasing carbon content from 0.03 to 0.11%

strength steel weld metals it was difficult to determine whether the microstructure was martensite or bainite owing to their similar morphologies.^{9,15} FEGSEM was therefore employed and proved to be a very revealing method. Investigations were carried out on all three samples, with only selected results presented here for the high and low carbon weld metals.

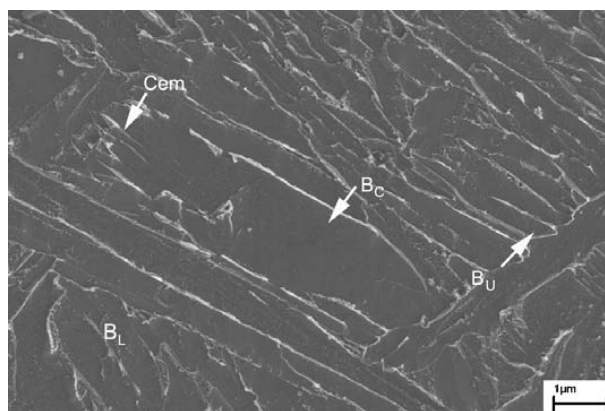
Images taken from the last bead in 7-0.5L200 are presented in Figs. 6 and 7. In agreement with LOM, the



5 Fine scale microstructure in last bead of low and high carbon weld metals (LOM)



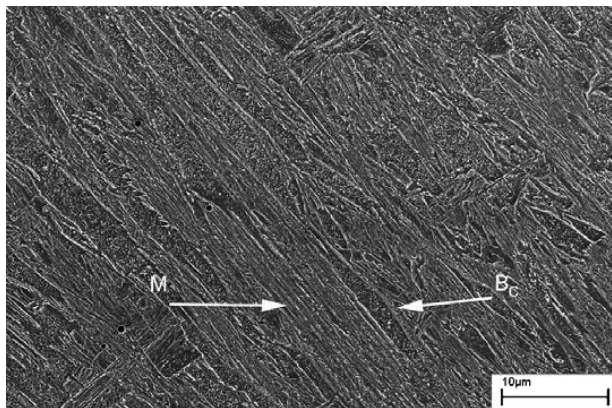
6 Microstructure of as deposited 7-0.5L200 weld metal, showing mainly upper bainite (B_U) together with coalesced bainite (B_C) found within former dendrites and predominantly laths of martensite (M) at interdendritic regions (FEGSEM)



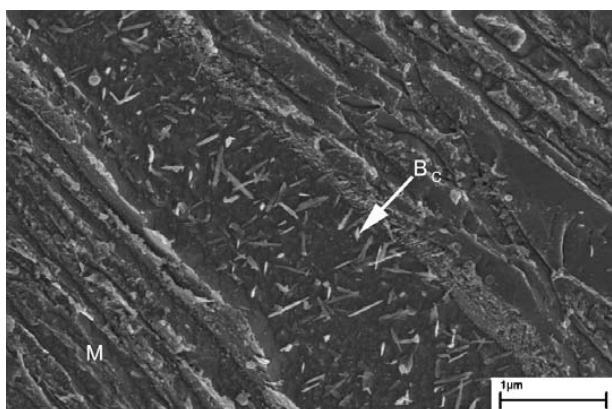
7 Upper bainite, lower bainite (B_L), and coalesced bainite within former dendrite at higher magnification in as deposited weld metal 7-0.5L200 (FEGSEM)

former dendritic structure that developed during solidification can be seen. A low magnification overview of the microstructure across a former dendrite is shown in Fig. 6. It can be seen that the microstructure varies in morphology across the region. When examinations were carried out at high magnification, it was commonly found that primarily bainite formed in the centre of the dendrites (Fig. 7) whereas a mixture of bainite and a lath like structure of martensite developed at the prior dendrite boundary regions. In bainitic areas cementite was mainly found at bainitic ferrite boundaries, giving upper bainite. A rather large grain is shown in Fig. 7, where a group of cementite platelets are penetrating the boundary tip. Cementite of this nature was also observed and characterised elsewhere in studies of coalesced bainite.^{12,16} Work on weld metals containing 7%Ni and 2%Mn showed that an unusual form of bainite developed. It had very large bainitic ferrite grains, without the typical subunit structure of platelets with cementite at boundaries. However, in the weld metals presented here the size of the coalesced bainite is considerably smaller.

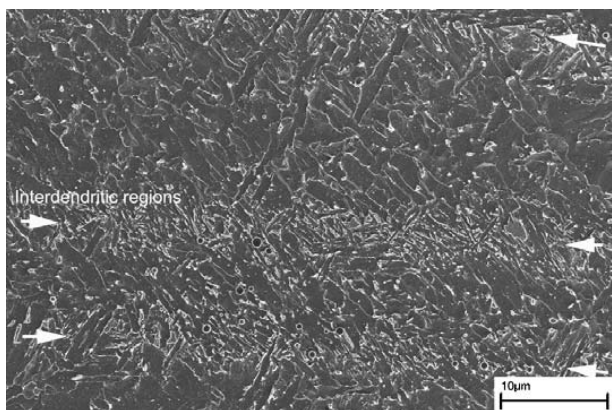
Figures 8 and 9 are FEGSEM images from the last bead of weld metal 7-0.5H200. A very fine scale microstructure was revealed (Fig. 8) and when examined at higher magnification found to be a mixture of mainly



8 Overview of as deposited weld metal 7-0.5H200, showing regions of martensite and coalesced bainite (FEGSEM)



9 Mixture of coalesced bainite and martensite in last bead of weld metal 7-0.5H200, at high magnification (FEGSEM)

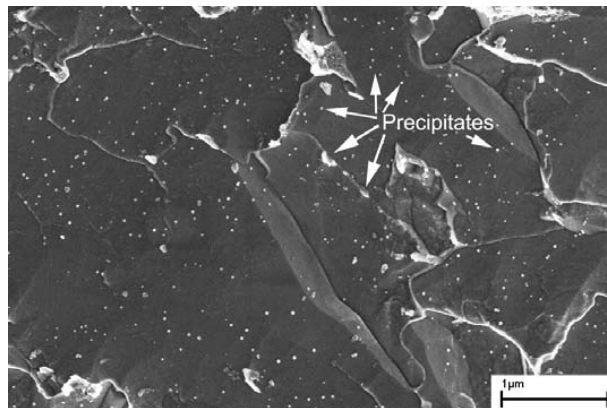


10 Overview of centre of reheated bead in 7-0.5L200 weld metal: former dendrite boundary regions are clearly visible (FEGSEM)

martensite with some coalesced bainite (Fig. 9). Lath shaped precipitates within grains, as shown in Fig. 9, were characterised to be cementite using TEM and electron diffraction. Similar cementite precipitates were found and identified also in a 7Ni-2Mn low carbon weld metal.¹²

Microstructure – reheated beads

The overall morphology in the centre of a reheated bead in weld metal 7-0.5L200 is shown in Fig. 10. In this



11 Microstructure of tempered bainite at centre of former dendrite in reheated bead in weld metal 7-0.5L200 (FEGSEM)

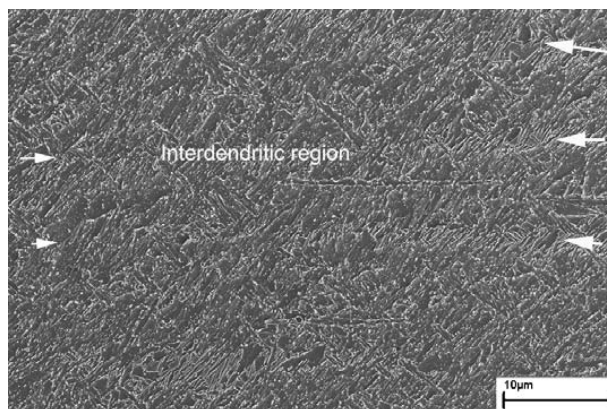
FEGSEM image it is possible to distinguish the former dendrite boundary regions. These regions show a finer microstructure, which is a mixture of tempered martensite and bainite. A comparatively coarse morphology of mainly tempered bainite was found in the dendrite core regions (Fig. 11). In both areas cementite precipitates were found at the boundaries and within the bainitic ferrite.

A FEGSEM overview of the centre of a reheated bead in weld metal 7-0.5H200 is shown in Fig. 12; the microstructure is generally much finer than in 7-0.5L200 (Fig. 10). Overall the microstructure was considered to be predominantly tempered martensite with some tempered bainite. A dendrite core region is shown in Fig. 13, where precipitates are found both at the boundaries and within the bainitic ferrite.

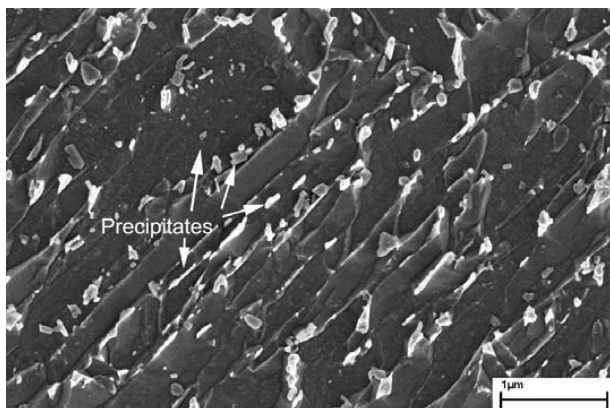
Dilatometry

The effect of carbon on the A_{c1} and A_{c3} temperatures was measured using dilatometry. It was found that the A_{c1} and A_{c3} temperatures were 685 and 770°C respectively for 7-0.5H200 measured at a heating rate of 25 K s⁻¹. These temperatures can be compared to values of 700 and 770°C for A_{c1} and A_{c3} for a low carbon weld metal similar to 7-0.5L200.¹⁰

Different cooling rates were selected to characterise the austenite decomposition temperatures in 7-0.5H200. For a cooling rate of 25 K s⁻¹ transformation occurred at 355°C and for a very low cooling rate of 1 K s⁻¹ the



12 Overview of microstructure in centre of reheated bead in weld metal 7-0.5H200 (FEGSEM)



13 Centre of dendrite at high magnification in reheated bead of weld metal 7-0.5H200 (FEGSEM)

transformation temperature was 365°C. These temperatures can be compared with results for low carbon content (0.03%) where transformation occurred at 490°C for a cooling rate of approximately 40 K s⁻¹ and at 480°C when cooling at 1 K s⁻¹.

Discussion

As expected carbon additions proved important not only for the mechanical properties but also for the microstructure in the 7Ni-0.5Mn system. It was found that carbon additions increased strength at limited expense to impact toughness. Microstructural investigations revealed a fine scale microstructure with martensite gradually replacing bainite as the dominant phase as carbon content increased from 0.03 to 0.11%.

In the low carbon weld metal a mixture of mainly upper bainite along with small amounts of lower and coalesced bainite developed in former dendrite core regions, whereas a fine microstructure of martensitic laths formed at the boundaries (Fig. 6). These differences are a consequence of the inevitable chemical segregation associated with the dendritic solidification. The segregation has previously been demonstrated experimentally; nickel and manganese are enriched in the interdendritic regions, where a greater quantity of martensite is found.^{10,11} Since both elements are austenite stabilisers, it follows that transformation at interdendritic regions occurs at lower temperatures thus promoting martensite.

It was observed that carbon additions also stabilise austenite to lower transformation temperatures. Transformation with 0.11%C occurred in the region of 355°C, some 125 K lower than for the 0.03%C weld metal, which transformed at about 480°C. It was decided to estimate the bainite start temperature B_S and martensite start temperature M_S using empirical equations^{17,18} for the average composition of the weld

metals (Table 1) to allow a comparison with the measured transformation temperatures. In the low carbon weld metal, B_S was estimated to be 498°C whereas M_S was predicted to be 395°C. Repeating the calculation for the high carbon weld metal, a B_S of 449°C and an M_S of 347°C were predicted. These predictions are not expected to be accurate since the equations do not extend to the present nickel concentrations. However, when calculated and measured transformation temperatures and the observed microstructure are compared, there is surprisingly good agreement (Table 2). The different microstructures observed suggest that the bainite nose in the continuous cooling transformation diagram is shifted to longer times at high carbon content.

Overall, it is found that increasing the carbon content enhances the formation of martensite and for a carbon content of 0.11%, martensite was the dominant phase not only at the former dendrite boundary regions, but also within the dendrites.

The microstructural changes that occurred were reflected in hardness measurements. The decrease in hardness in the 0.03%C weld metal as reheated regions were encountered may be explained by redistribution of carbon in the bainitic ferrite platelets along with the coarsening and spheroidising of cementite. In tempered martensitic regions it was also found that precipitation occurred, with the formation of cementite. The formation of precipitates and the loss of carbon in solid solution results in a marked decrease in hardness. As a consequence the greatest hardness reduction was observed for the predominantly martensitic high carbon weld metal.

The gradual increase in strength due to carbon additions could be attributed to the increase in the proportion of martensite. Martensite gives a smaller effective grain size, which is inherited on tempering and contributes to strength and explains the limited loss of impact toughness.

Conclusions

As predicted by neural network modelling, carbon additions from 0.03 to 0.11 wt-% in high strength steel weld metals with 7%Ni and 0.5%Mn were found to have a positive effect on strength at minor expense to toughness.

With low carbon content, different types of bainite were characterised using FEGSEM at former dendrite core regions, whereas a lath like microstructure of martensite was found at interdendritic regions. These differences were attributed to segregation of manganese and nickel. As carbon content increased austenite was stabilised to lower transformation temperatures and gradually the microstructure became predominantly martensitic in nature.

Carbon additions were found to promote martensite, resulting in a harder and stronger microstructure. The

Table 2 Comparison between transformation temperature measured using dilatometry and transformation temperatures predicted using empirical equations^{17,18} for bainite (B_S) and martensite (M_S) for high and low carbon weld metals

Weld metal	Main constituent	Measured transformation temperature, °C	Calculated transformation temperature, °C	
			M_S	B_S
Low carbon	Bainite	490	395	498
High carbon	Martensite	355	347	449

relatively minor reduction in impact toughness as strength increased was attributed to the overall refinement of the microstructure.

Acknowledgements

Professor L.-E. Svensson of Chalmers University of Technology is thanked for fruitful discussions. Mr P. Lindström of Sandvik Technology is gratefully acknowledged for help with dilatometry experiments. ESAB AB is thanked for the production of experimental weld metals, permission to publish results, and financial support. The Knowledge Foundation of Sweden is thanked for additional financial support.

References

1. J. J. Deloach, C. Null, S. Fiore and P. Konkol: *Weld. J.*, 1999, **78**, (6), 55–58.
2. L.-E. Svensson: *Svetsaren*, 1999, **54**, 29.
3. D. J. Widgery, L. Karlsson, M. Muruganath and E. Keehan: 'Approaches to the development of high strength weld metals', Proc. 2nd Int. Symp. on 'High strength steel', Verdal, Norway, April 2002, SINTEF Materials Technology.
4. Y. Kang, H. J. Kim and S. K. Hwang: *ISIJ Int.*, December 2000, **40**, 1237.
5. D. J. C. Mackay: *Neural Comput.*, 1992, **4**, (3), 448.
6. D. J. C. Mackay: *Neural Comput.*, 1992, **4**, (3), 415.
7. H. K. D. H. Bhadeshia: *ISIJ Int.*, October 1999, **39**, 966.
8. M. Muruganath, H. K. D. H. Bhadeshia, E. Keehan, H. O. Andrén and L. Karlsson: 'Strong and tough ferritic steel welds', in 'Mathematical modelling of weld phenomena 6' (ed. H. Cerjak), 205–230; 2002, Abington, Woodhead.
9. Z. Zhang and R. A. Farrar: *Weld. J.*, 1997, **76**, (5), 183s–196s.
10. E. Keehan, L. Karlsson, H. O. Andrén and H. K. D. H. Bhadeshia: *Sci. Technol. Weld. Joining*, 2006, **11**, (1), 9–18.
11. E. Keehan, L. Karlsson and H. O. Andrén: *Sci. Technol. Weld. Joining*, 2006, **11**, (1), 1–8.
12. E. Keehan: PhD thesis, Paper 3, Chalmers University of Technology, Gothenburg, Sweden, 2004.
13. E. Keehan: PhD thesis, Paper 7, Chalmers University of Technology, Gothenburg, Sweden, 2004.
14. 'WeldCalc' software, Version 1.0.0, SSAB, Oxelösund, Sweden, 1998–1999.
15. T. Araki, M. Enomoto and K. Shibata: *Mater. Trans. JIM*, 1991, **32**, (8), 729.
16. H. K. D. H. Bhadeshia: 'Theory and significance of retained austenite in steels', PhD thesis, University of Cambridge, Cambridge, UK, 1979.
17. R. W. K. Honeycombe and H. K. D. H. Bhadeshia: 'Steel microstructure and properties', 2nd edn, 133; 1995, London, Edward Arnold.
18. R. W. K. Honeycombe and H. K. D. H. Bhadeshia: 'Steel microstructure and properties', 2nd edn, 103; 1995, London, Edward Arnold.